Developmental Biology 351 (2011) 13–24

Contents lists available at ScienceDirect

Developmental Biology

journal homepage: www.elsevier.com/developmentalbiology

Protogenin mediates cell adhesion for ingression and re-epithelialization of paraxial mesodermal cells

Kodai Ito [a], Harukazu Nakamura [a,b], Yuji Watanabe [a,b,*]

[a] Department of Molecular Neurobiology, Graduate School of Life Sciences, Tohoku University, 4-1 Seiryo-machi. Aoba-ku, Sendai 980-8575, Japan
[b] Institute of Development, Aging and Cancer, Tohoku University, Japan

ARTICLE INFO

Article history:
Received for publication 23 July 2010
Revised 10 November 2010
Accepted 19 November 2010
Available online 1 December 2010

Keywords:
Ingression
Migration
Paraxial mesoderm
Adhesion
Chick

ABSTRACT

In the avian embryo, precursor cells of the paraxial mesoderm that reside in the epiblast ingress through the primitive streak and migrate bilaterally in an anterolateral direction. Herein, we report on the roles of Protogenin (PRTG), an immunoglobulin superfamily protein expressed on the surface of the ingressing and migrating cells that give rise to the paraxial mesoderm, in paraxial mesoderm development. An aggregation assay using L-cells showed that PRTG mediates homophilic cell adhesion. Overexpression of PRTG in the presumptive paraxial mesoderm delayed mesodermal cell migration due to augmented adhesiveness. In contrast, siRNA knockdown of PRTG impaired successive ingression of epiblast cells and disorganized the epithelial structure of the somites. These results suggest that PRTG mediates cell adhesion to regulate continuous ingression of cells giving rise to the paraxial mesodermal lineage, as well as tissue integrity.

Introduction

Early morphogenetic movements include the active cell rearrangements of mesodermal cells. In mammals and birds, presumptive mesodermal cells residing in the epiblast ingress through the primitive streak. These cells undergo epithelial–mesenchymal transformation (EMT) to leave the epiblast layer. Internalized mesodermal cells migrate further in an anterolateral direction to form the paraxial, intermediate and lateral plate mesoderm (Ooi et al., 1986; Schoenwolf et al., 1992; Psychoyos and Stern, 1996; Catala et al., 1996; Wilson and Beddington, 1996; Iimura et al., 2007). In the paraxial mesodermal lineage, migrating mesenchymal cells form a bilateral array comprised of presomitic mesoderm, which is re-epithelialized periodically upon segmentation along the anteroposterior axis to form epithelial somites.

Recent studies suggest that cell adhesion coordinates cell movements in early embryogenesis (Hammerschmidt and Wedlich, 2008). For example, the cell–cell adhesion molecule such as E-cadherin is expressed in epithelial cells before the cells undergo EMT, and helps maintain epithelial integrity under the control of fibroblast growth factor (FGF) signaling (Larue et al., 1994; Burdsal et al., 1993; Ciruna and Rossant, 2001). On the other hand, N-cadherin is crucial for mesodermal migration by allowing mesodermal cells to gain the traction necessary for migration (Yang et al., 2008). In addition, N-cadherin has been demonstrated to be necessary for mesodermal morphogenesis (Radice et al., 1997; Warga and Kane, 2007).

Protogenin (PRTG) is a membrane protein of the immunoglobulin superfamily (IgSF). It contains four extracellular immunoglobulin domains and five fibronectin III domains, making it structurally related to deleted in colorectal cancer (DCC) and Neogenin, which are receptors for Netrin1 and RGMa, respectively, as well as to cell adhesion molecules such as L1 and neural cell adhesion molecule (NCAM). We have reported previously on the expression pattern of *prtg* in early chick embryos, demonstrating *prtg* expression in the neural tube and paraxial mesoderm (Toyoda et al., 2005). Similar expression patterns for *prtg* have been reported in the mouse and zebrafish, suggesting a conserved role for *prtg* among species (Vesque et al., 2006). Specific expression of *prtg* in the paraxial mesodermal lineage prompted us to investigate the function of PRTG, in particular in mesodermal formation, including ingression of the epiblast, migration of the paraxial mesodermal cells, and subsequent somitogenesis.

In the present study, we show that PRTG augments the cell adhesive properties of cultured L-cells. In chick embryos, PRTG protein is localized at the site of contact between epiblast cells and cells undergoing ingression and migration. Following PRTG overexpression in chick embryos, the PRTG-overexpressing cells formed aggregates in the paraxial mesoderm, indicating that PRTG mediates adhesion in vivo, and mesodermal cell migration was delayed. Knockdown of PRTG by siRNA disrupted both the continuous ingression and the formation of the paraxial mesoderm, although mesodermal cell migration was not affected. These data suggest that PRTG mediates cell adhesion to coordinate movement and tissue integrity in the paraxial mesodermal lineage.

* Corresponding author. Department of Molecular Neurobiology, Graduate School of Life Sciences, Tohoku University, 4-1 Seiryo-machi. Aoba-ku, Sendai 980-8575, Japan. Fax: +81 22 717 8554.
E-mail address: yuji@idac.tohoku.ac.jp (Y. Watanabe).

0012-1606/$ – see front matter © 2010 Elsevier Inc. All rights reserved.
doi:10.1016/j.ydbio.2010.11.024

Methods

Constructions for PRTG gain- and loss-of-function experiments

Full-length cDNA of the coding region of chick *prtg* (Genbank AB185923; Toyoda et al., 2005) was amplified with C-terminal c-myc tag by PCR and subcloned into pCAGGS vector (pCAGGS-PRTG).

Double-stranded siRNA for *prtg* (siPRTG) and five-base mismatched double-stranded RNA (control siRNA) were synthesized with TT overhang (Nihon gene research laboratories, Sendai, Japan). The sequences of the siPRTG and control siRNA were GGAUCUACACCUUAUCCAAUG and GGAUGUAGACGUUAUCGAAUC, respectively.

For rescue siRNA experiment, *prtg* cDNA with synonymous substitutions in the target sequence of siPRTG (GGATCTATACGCTGTCGAATG) was amplified by PCR and then subcloned into a pCAGGS vector (pCAGGS-PRTGmut). We confirmed that PRTG expression from pCAGGS-PRTGmut was not altered by siPRTG.

Electroporation and whole embryo culture

For *prtg* transfection, pCAGGS-PRTG (5.0 μg/μl) and pCAGGS-EGFP (5.0 μg/μl) were co-electroporated. As a control, mock pCAGGS vector (5.0 μg/μl) and pCAGGS-EGFP (5.0 μg/μl) were co-electroporated. For siRNA experiments, either siPRTG or control siRNA (1.0 μg/μl) was mixed with pCAGGS-EGFP (5.0 μg/μl) and electroporated. For rescue experiments, pCAGGS-PRTGmut (0.3 μg/μl) was mixed with siPRTG (1.0 μg/μl) and pCAGGS-EGFP (4.0 μg/μl).

In ovo electroporation into the epiblast of the presumptive paraxial mesoderm was performed as described by Sato et al. (2002). Briefly, the DNA solution was placed onto the anterior primitive streak, and a cathode (needle shaped) was placed into the DNA solution. A stick-type anode electrode was placed beneath the embryo (Fig. 3D, E). An electric pulse (6 V, 25 ms) was applied three times at 975 ms intervals using CUY21 electroporator (BEX, Tokyo, Japan).

In vitro electroporation and whole embryo culture were performed according to the methods described by Hatakeyama and Shimamura (2008). Briefly, stage 6 embryos (Hamburger and Hamilton, 1951) were attached to filter paper and placed in a Petri dish containing a square electrode at its center (CUY701P2E; Unique Medical Imada, Natori, Japan). The Petri dish was filled with simple saline solution. Electroporation was performed using three electric pulses (6 V, 50 ms) applied at 100 ms intervals. Embryos were then cultured in albumen-based 35 mm glass-bottomed dish (Matsunami Glass, Osaka, Japan) at 38 °C in a humid atmosphere (EC culture; Chapman et al., 2001).

Time-lapse imaging and data analysis

An embryo in EC culture was placed in the chamber unit that was set on an inverted microscope (IX81, Olympus, Tokyo, Japan) and supplied with 5% CO_2 flow (Control Unit MIGM/OL, Tokai Hit, Shizuoka, Japan) with temperature control at 38 °C (MI-IBC, Olympus). Confocal GFP fluorescence images and DIC (differential interference contrast) images were captured with a microscope (FV300, Olympus) every 5 μm along *Z*-axis for 60 μm depth. *Z*-stack images of every 5 min during 12 h were collected to reconstruct time-lapse movie.

Cell adhesion assay

Full-length chick *prtg* cDNA was subcloned into pT2K-CAGGS vector. Subsequently, the neomycin gene cassette (SV40 early promoter/Neo/SV40 early polyA signal) was amplified by PCR from pcDNA3.1 (Invitrogen) and inserted to establish a pT2K-Neo-CAGGS-PRTG vector. The pT2K-Neo-CAGGS-EGFP vector was obtained by replacing CAGGS-PRTG with enhanced GFP (EGFP) cDNA from pEGFP-N1. The pT2K-Neo-CAGGS-EGFP or pT2K-Neo-CAGGS-PRTG vectors were transfected into L-cells with the tol2 transposase construct pCAGGS-T2TP (Sato et al., 2007) using Targefect F-2 transfection reagent (Targeting Systems, El Cajon, CA). Stable cell lines from a single clone expressing EGFP or PRTG were established after selection with G418 (500 μg/ml) for 2 weeks.

L-Cells stably expressing EGFP or PRTG were incubated with 2 mM EDTA/PBS(-) for 15 min at room temperature and dissociated from the dish by gentle pipetting. Cells were suspended in Dulbecco's modified Eagle's medium (DMEM) containing 10% fetal bovine serum (FBS) at a density of 1.0×10^6 cells/ml and subsequently transferred to 12-multiwell plates of low cell attachment (HydroCell, CellSeed, Tokyo, Japan). Plates were placed on a shaker and cells were rotated at 80 r.p.m. at 37 °C to form aggregates. Total particle number (Nt) and the number of aggregates with more than three cells were determined every 15 min using a hemocytometer.

For the mixed cell aggregation assay, PRTG-expressing cells were labeled with PKH red fluorescent dye according to the manufacturer's instructions (Sigma-Aldrich). Equal numbers of EGFP- and PRTG-expressing cell lines were mixed and rotated at 80 r.p.m. at 37 °C for 60 min. Aggregates were subjected to confocal laser scanning microscopy to count the number of red or green fluorescent cells. For each cell aggregate with more than three cells, the number of PRTG-expressing cells per total cell number was calculated.

For the cell–extracellular matrix (ECM) adhesion assay, dissociated L-cells stably expressing EGFP or PRTG were transferred to six-well plates coated with mouse collagen IV, human fibronectin, or mouse laminin (BD Biosciences). After incubation at 37 °C for 10 min (collagen IV, fibronectin) or 30 min (laminin), cells were washed twice with phosphate-buffered saline (PBS) to count the number of adherent cells on ECM-coated plates.

Antibody production

For the production of rabbit polyclonal antibodies against PRTG, cDNA coding the intracellular domain of chick PRTG (amino acids 964–1187) was subcloned into pET102 (Invitrogen) to generate a fusion protein tagged with six histidine residues at its C-terminal. After transfection to *Escherichia coli* BL21 Star and isopropylthio-β-galactoside (IPTG) induction, the protein was purified using an Ni-NTA purification system (Invitrogen) before being used as the antigen. Rabbits were immunized six times (Medical and Biological Laboratories, Nagoya, Japan), and the antisera raised were purified using HiTrap Protein A HP column (GE).

The specificity of the antibody was confirmed by western blotting using gradient SDS-PAGE (5–20% gel) for homogenized embryonic day 2 (E2) embryos or cultured 293 T cells transfected with full-length chick PRTG cDNA. The purified antibody for PRTG detected a single band that was slightly greater than the predicted PRTG protein (128 kDa), which may be due to glycosyl modification (Supplementary Fig. 1).

In situ hybridization and immunostaining

Whole-mount in situ hybridization was performed as described previously (Henrique, 1997; Toyoda et al., 2005). For immunohistochemistry, cryosections were reacted with 1/1000 diluted anti-PRTG polyclonal antibody and 1/400 diluted Alexa594-labeled anti-rabbit IgG (Invitrogen). The GFP signal was enhanced using 1/1000 diluted anti-GFP polyclonal antibody (Invitrogen) or 1/400 diluted anti-GFP monoclonal antibody (Wako, Osaka, Japan) with an Alexa488-labeled secondary antibody (Invitrogen).

Fluorescent images were captured using confocal laser scanning microscopy (FV300, Olympus) or with a cooled CCD digital camera (ORCA-ER, Hamamatsu, Japan).

Results

PRTG mediates cell adhesion

Because PRTG is a membrane protein that is structurally related to the cell adhesion molecules, a possible function of PRTG as a cell adhesion molecule was investigated in the present study using cell aggregation assay with L-cells that stably expressed PRTG. Most control L-cells remained dissociated after 75 min rotation culture (Fig. 1A). In contrast, PRTG-expressing L-cells in rotation culture formed a number of aggregates composed of more than three cells (Fig. 1B). The number of aggregates formed increased linearly with incubation time (Fig. 1C). Concomitantly, the ratio of total particle numbers to the initial particle number (Nt/No) decreased linearly with incubation time (Fig. 1D). This time-dependent enhancement of aggregation indicates that PRTG augments adhesion of L-cells.

Next, a mixed cell aggregation assay using an equal number of control and PRTG-expressing L-cells was performed. The control and PRTG-expressing L-cells emit green or red fluorescence, respectively (Fig. 1F). The proportion of PRTG-expressing cells in aggregates was determined (Fig. 1G). In most aggregates, the proportion of PRTG-expressing cells exceeded 50% (Fig. 1G), and PRTG-expressing cells were juxtaposed (Fig. 1F), suggesting strong preference for homophilic binding.

The effects of PRTG on interactions between L-cells and the ECM were examined because ECM components, such as collagen, fibronectin, and laminin, associate with paraxial mesodermal cells and play a role in morphogenesis (Bellairs, 1979; Rifes et al., 2007; Nakaya et al., 2008). Adhesion of PRTG-expressing L-cells to ECM-coated plates (collagen IV, fibronectin, and laminin) was comparable to that of control L-cells, indicating that PRTG does not affect the interaction between the cells and these ECM components (Fig. 1H).

PRTG is expressed on the cell surface of cells of the paraxial mesodermal cell lineage

Previously, we showed that *prtg* is expressed in mesodermal cells in early chick embryos (Toyoda et al., 2005). In the present study, we confirmed the expression of *prtg* in cells of the mesodermal cell lineage. In stage 7 embryos, *prtg* mRNA was expressed in the caudal half of the embryo, posterior to Hensen's node (Fig. 2A). Transverse sections showed that *prtg* was expressed in the epiblast and in the mesodermal cells at the level of the primitive streak (Fig. 2C), whereas Hensen's node, which eventually forms the notochord, was devoid of *prtg* expression (Fig. 2B). At stage 8, *prtg* expression became prominent in the paraxial mesoderm and neural plate (Fig. 2D). Both presomitic and somitic mesoderm cells were *prtg* positive, whereas the notochord was negative (Fig. 2E, F). In the epiblast, cells of the prospective paraxial mesoderm region express *prtg* before they ingress. After ingression, *prtg* expression may be maintained in paraxial mesodermal cells while they are in the presomitic mesoderm, and subsequently, in the somite.

The distribution of PRTG protein in prospective mesodermal cells was evaluated immunohistochemically. In accordance with the results obtained using in situ hybridization, PRTG was localized to the epiblast cells, ingressing cells, and already ingressed mesodermal cells (Fig. 2G). In the epiblast, PRTG was preferentially localized on the cell surface, especially at the sites of tight cell–cell contact (Fig. 2H). After ingression, mesodermal cells are still associated with one another, although the areas of membrane apposition are decreased. In these cells, PRTG was localized to the site of cell–cell contact (Fig. 2I). Similar PRTG localization was observed in the paraxial mesoderm and in the somites (Fig. 2J, K). These findings indicate that prospective paraxial mesodermal cells retain PRTG on their surface before and during ingression, migration, and somitogenesis.

PRTG-overexpression results in cell aggregates in the paraxial mesoderm

Cells of the paraxial mesodermal lineage expressed PRTG prior to ingression and after the formation of somites. PRTG was localized to the cell surface at the sites of cell–cell contact. Taking into consideration the fact that PRTG augmented the adhesion of L-cells, we assumed that PRTG mediates adhesion during processes of cell rearrangement, such as during the ingression and migration of cells of the paraxial mesodermal lineage, by allowing them with the traction necessary for migration. In order to assess this assumption, we overexpressed PRTG in presumptive mesodermal cells in the epiblast layer. At the six-somite stage, the fate map of the epiblast posterior to Hensen's node is (from the rostral to caudal) prospective neural tube, followed by paraxial, intermediate, and lateral plate mesoderm (Psychoyos and Stern, 1996; Catala et al., 1996). Epiblast cells of the presumptive paraxial region ingress through the primitive streak, migrate bilaterally in an anterolateral direction (Fig. 3A, B), and eventually form the paraxial mesoderm (i.e., the presomitic mesoderm and the somite; Fig. 3C). We electroporated PRTG expression construct at six-somite stage into the epiblast, which eventually contributes to the paraxial mesoderm (Fig. 3D, E).

In control embryos, into which a GFP expression construct was electroporated, GFP-positive cells were located in the presomitic mesoderm and the caudal-most somites (Fig. 3F). Five caudal-most somites contained more than 10 GFP-expressing cells after 28 h of electroporation (Fig. 3H). However, when PRTG was overexpressed, transfected cells, assessed by GFP expression, were also located in the presomitic mesoderm and the somite, but the anterior limit of GFP-expressing cells was posterior to that seen in control embryos (Fig. 3G), that is, two caudal-most somites contained more than 10 GFP-expressing cells after 28 h of electroporation (Fig. 3H). There was no significant difference in the total number of somites between the control and PRTG-overexpressing embryos, indicating that PRTG-overexpression does not impair somitic segmentation (Fig. 3I). However, the size of the somite in PRTG-transfected embryos was smaller than that in the control group (Fig. 3J).

In transverse sections, GFP-positive cells in control embryos were distributed ubiquitously in a patched pattern in both the presomitic mesoderm and somite (Fig. 4A–D). In PRTG-transfected embryos, transfected cells formed aggregates, with most aggregates located in the ventral part of the presomitic mesoderm and somite (Fig. 4E–H). A ventrally condensed distribution of PRTG-transfected cells was obvious in sagittal sections across the presomitic mesoderm and somite (Fig. 4I–L). In the aggregates formed by PRTG-transfected cells, overexpressed PRTG was found to be condensed at the sites of cell contact (Fig. 4M-O). These results support the notion that overexpression of PRTG increases the adhesiveness of cells of the paraxial mesodermal lineage.

PRTG loss-of-function impairs ingression of the epiblast

To investigate the effects of loss-of-function, siRNA was used to knockdown PRTG. To obtain effects rapidly, we electroporated short double-stranded RNA instead of the short hairpin (sh) RNA expression vector. By 6 h after electroporation, knockdown of *prtg* by siPRTG was obvious (Fig. 5C, D). Using control siRNA with a five-base mismatch had no effect on *prtg* mRNA expression (Fig. 5A, B).

Twelve hours after electroporation, a dorsal view of control embryos showed that GFP-positive cells were ingressed and dispersed anterolaterally (Fig. 5E). In contrast, in PRTG-knockdown embryos, GFP-positive cells were crowed near the primitive streak (Fig. 5J). In transverse sections of control embryos, many GFP-positive cells were seen to have already ingressed and dispersed beneath the epiblast by 12 h after electroporation (Fig. 5F–I). However, in PRTG-knockdown embryos, GFP-positive cells were located in the epiblast and mesodermal layer. In the epiblast of PRTG-knockdown embryos, it

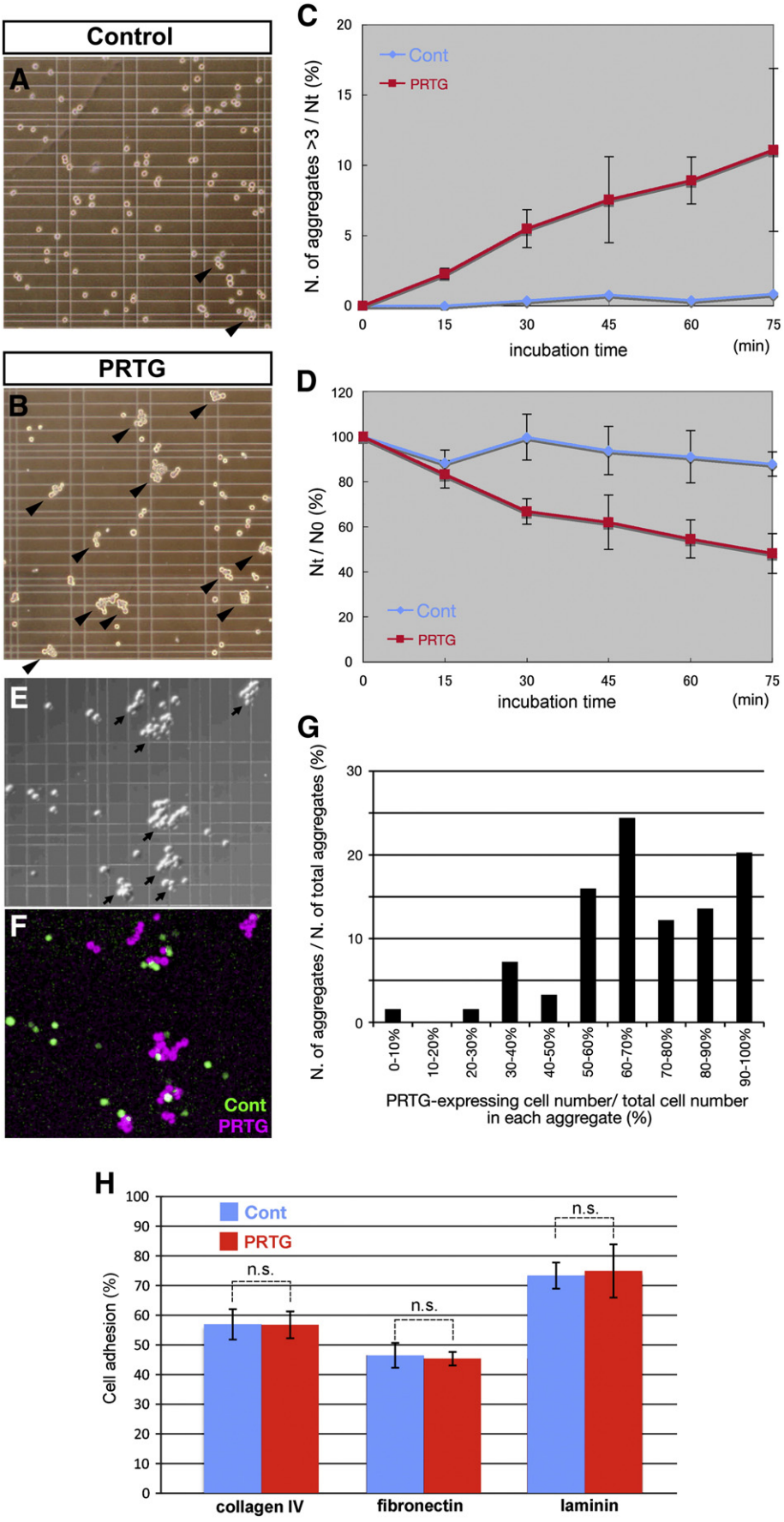
Control
A
PRTG
B
C
N. of aggregates >3 / Nt (%)
Cont
PRTG
incubation time
(min)
D
Nt / N0 (%)
Cont
PRTG
incubation time
(min)
E
F
Cont
PRTG
G
N. of aggregates / N. of total aggregates (%)
0-10%
10-20%
20-30%
30-40%
40-50%
50-60%
60-70%
70-80%
80-90%
90-100%
PRTG-expressing cell number/ total cell number in each aggregate (%)
H
Cell adhesion (%)
Cont
PRTG
n.s.
n.s.
n.s.
collagen IV
fibronectin
laminin

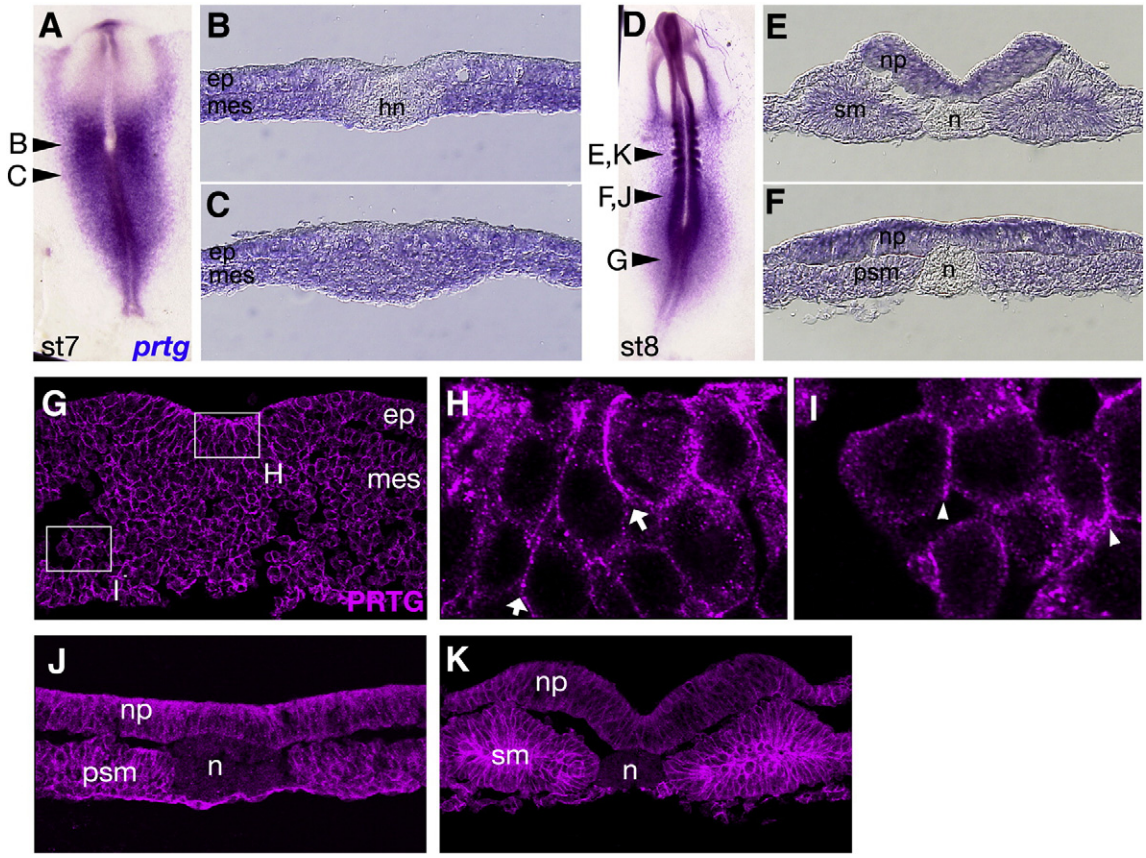

Fig. 2. Expression of *prtg* mRNA (A–F) and Protogenin (PRTG) protein (G–K) in chick embryos. (A, D) Dorsal view of *prtg* mRNA expression at stage 7 and 8 embryos. Arrowheads indicate the levels of transverse section. (B, C; E, F) Distribution of *prtg* mRNA in transverse sections. (G-K) Immunohistochemistry of anti-PRTG antibody with confocal laser scanning microcopy. (H; I) Higher magnification of the area denoted by boxes in (G). Note PRTG localizes on plasma membrane, especially at the site of cell–cell contact between epiblast cells (H; arrows) and mesenchymal cells (I; arrowheads). ep, epiblast; mes, mesoderm; hn, Hensen's node; np, neural plate; sm, somite; n, notochord; psm, presomitic mesoderm.

appeared that the ingression of the cells was impaired and the cells had accumulated near the primitive streak (Fig. 5K–N). Next we tried to observe the morphology of the transfected cells in the epiblast, to examine the polarized morphology of the ingressing cells observed by electron microscopy (Bancroft and Bellairs, 1975). Because the individual cell shape was obscure under fluorescent microscopy, we used confocal microscopy, which enables a detailed analysis of the cell shape at a focal plane. In control embryo, ingressing cells on the apical side of the epiblast displayed a typical bottle shape (Fig. 5O, P; Bancroft and Bellairs, 1975). In contrast, in PRTG-knockdown embryos the transfected cells exhibited a round morphology instead of a polarized shape (Fig. 5Q, R). We confirmed that apoptotic cell death was not induced by PRTG-knockdown using anti-Caspase3 staining (data not shown).

To clarify actual cellular movement, we captured time-lapse images of DIC and GFP fluorescence in whole embryo culture (Fig. 6; Movies 1, 2). Because of the embryonic extension at this stage, the fluorescence mass moved caudally in both control and PRTG-knockdown embryos. In control embryos, GFP-positive cells in the epiblast first moved medially towards the primitive streak, which could be inferred by solid fluorescence (Movie 1). Several hours later, cells with dim GFP fluorescence, which were assumed to be ingressed paraxial mesodermal cells, migrated out bilaterally (Fig. 6B, white enclosure). Later, individual GFP-positive cells or small groups of GFP-positive cells were seen to move anterolaterally to join the array of the paraxial mesoderm, which was elongated rostrocaudally (Movie 1; Fig. 6C, D, white enclosure). In PRTG-knockdown embryos, GFP-positive cells remained in the epiblast layer (Movie 2, Fig. 6E–H, black arrow), as seen in transverse sections (Fig. 5K). Some of the cells in PRTG-knockdown embryos had ingressed and joined the paraxial mesoderm (Fig. 6G, H, white enclosure), but the number of cells in the paraxial mesodermal array was less than in control embryos and the array was narrower. These results indicate that loss-of-function for PRTG impairs the ingression of precursor cells of the paraxial mesoderm in the epiblast.

Fig. 1. Cell aggregation assay. (A, B) Single-cell suspensions of L-cells stably expressing enhanced green fluorescent protein (GFP) or Protogenin (PRTG) were rotated to form aggregates. Cell aggregation of EGFP-transfected (A: Control) or PRTG-transfected (B: PRTG) L-cells after 75 min incubation is shown. Arrowheads indicate cell aggregates with more than three cells. (C, D) Time course of the formation of cell aggregates by EGFP-transfected (blue circles) or PRTG-transfected (red squires) L-cells. The ratio of the number of aggregates with more than three cells to the total particle number at time *t* of incubation (*Nt*) is shown in (C), whereas the ratio of the total particle number at time *t* of incubation (*Nt*) to the initial particle number (*No*) is shown in (D). The number of particles was counted every 15 min using a hemocytometer. Error bars indicate standard errors. (E–G) Mixed cell aggregation assay between EGFP-transfected (green) and PRTG-transfected (magenta) L-cells. (E, F) Differential interference contrast (DIC) and fluorescent images of the mixed cell aggregation assay. Arrows indicate cell aggregates with more than three cells. PRTG-transfected L-cells segregate in the aggregates from less number of control L-cells. (G) Ratio of the number of aggregates to the total number of aggregates after 60 min incubation plotted according to the composition of PRTG-transfected cell number per total cell number in each cell aggregate ($n = 582$). (H) The ratio of cell adhesion to different extracellular matrix components was compared between EGFP-transfected (blue) or PRTG-transfected (red) L-cells. Error bars indicate the standard deviation. n.s., not significant (by *t*-test).

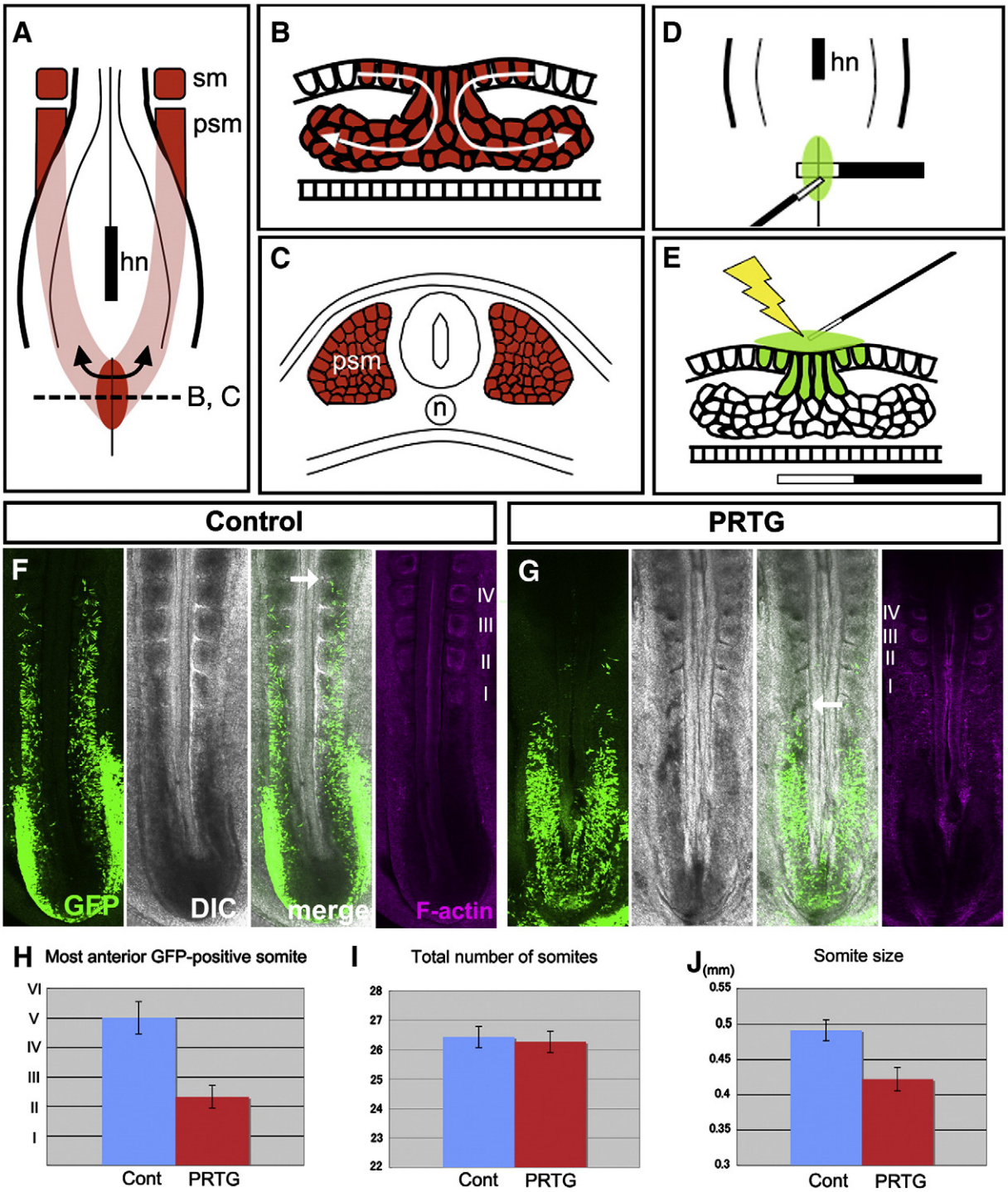

Fig. 3. Protogenin (PRTG) overexpression in the mesoderm precursors in the epiblast. (A–C) Schematic drawings of cell movement of the presumptive paraxial mesoderm. (A) Dorsal view of a six-somite stage embryo showing the cell migration stream of the presumptive paraxial mesoderm in red. The epiblast cells of the presumptive paraxial mesoderm (red area at the midline) are located in the anterior primitive streak, posterior to Hensen's node (hn). After ingression, they migrate in an anterolateral direction (arrows) to form the presomitic mesoderm (psm) and eventually the somites (sm). (B, C) Transverse sections at the level denoted in (A), 6 h and 1 day later, respectively. The epiblast cells ingress at the primitive streak moving ventrally, and undergo epithelial–mesenchymal transformation. They subsequently migrate laterally (B; white arrows), and eventually form the presomitic mesoderm (C). (D, E) Schematic drawings of electroporation into the epiblast in the dorsal view (D) and transverse (E) view. The DNA solution was placed on the epiblast and electroporated with a needle-type cathode electrode on the epiblast and a baton-type anode electrode beneath the embryo. n, notochord. (F, G) Distribution of GFP (green), F-actin (magenta) and an image showing differential interference contrast (black and white) in GFP-transfected embryos (F) or GFP- and PRTG- transfected embryos (G) 28 h after electroporation. Confocal Z-stack images are shown. White arrows indicate the anterior limit of GFP-positive somites. Roman numerals indicate somite number from newly segmented somites. (H) The most anterior somite containing a GFP-positive cell population of more than 10 cells. Cont, EGFP-transfected control ($n=14$), PRTG, PRTG and EGFP-transfected ($n=18$). (I) Total number of the somites 28 h after electroporation in Cont ($n=14$) and PRTG ($n=18$) groups. (J) The length of the last three somites (I, II and III) along the anterior-posterior axis in Cont ($n=14$) and PRTG ($n=17$) groups.

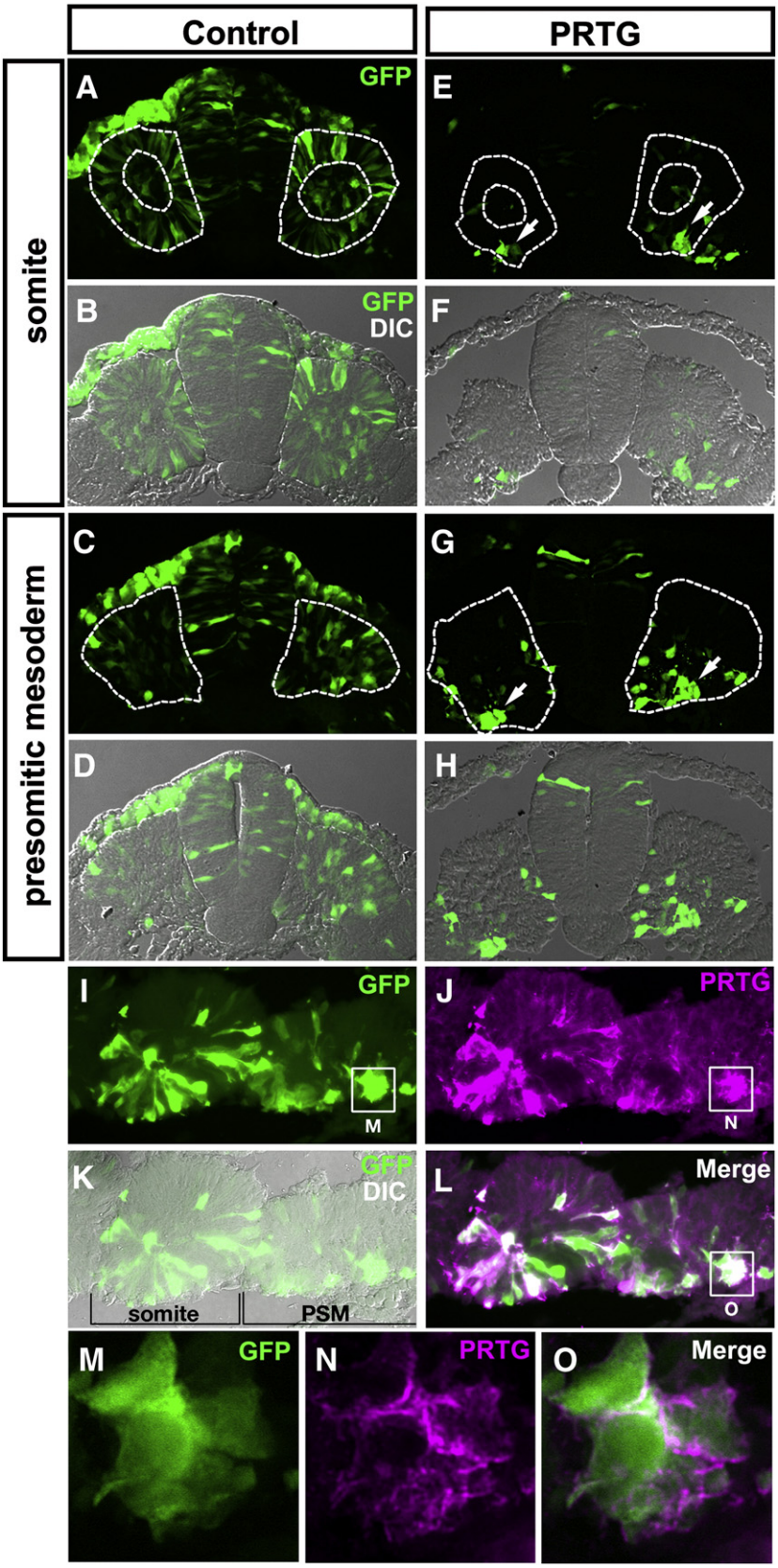

Fig. 4. Cell aggregation in the paraxial mesoderm after Protogenin (PRTG) overexpression. (A–H) Distribution of GFP-transfected (A–D) or GFP- and PRTG-transfected (E–H) mesodermal cells in transverse section at the level of somites (A, B; E, F) or presomitic mesoderm (C, D; G, H) 28 h after electroporation. Although GFP-transfected cells were dispersed throughout the entire somite and presomitic mesoderm (A, C; nine similar phenotypes from nine independent experiments), PRTG-transfected cells accumulated in the ventral part of the paraxial mesoderm (E, G; arrows; six similar phenotypes from nine independent experiments). White doted lines indicate the area of the somite and the presomitic mesoderm (A, C; E, G). (I–L) Sagittal section of GFP- and PRTG-transfected paraxial mesoderm across the somite and the presomitic mesoderm (PSM). Anterior is left. GFP-transfected cells expressing an excess of PRTG accumulated in the ventral part of the somite and PSM and formed aggregates. (M–O) Higher magnification of the area denoted by the boxes in (I, J, L). Transfected PRTG was prominent on the plasma membrane at sites of cell–cell adhesion.

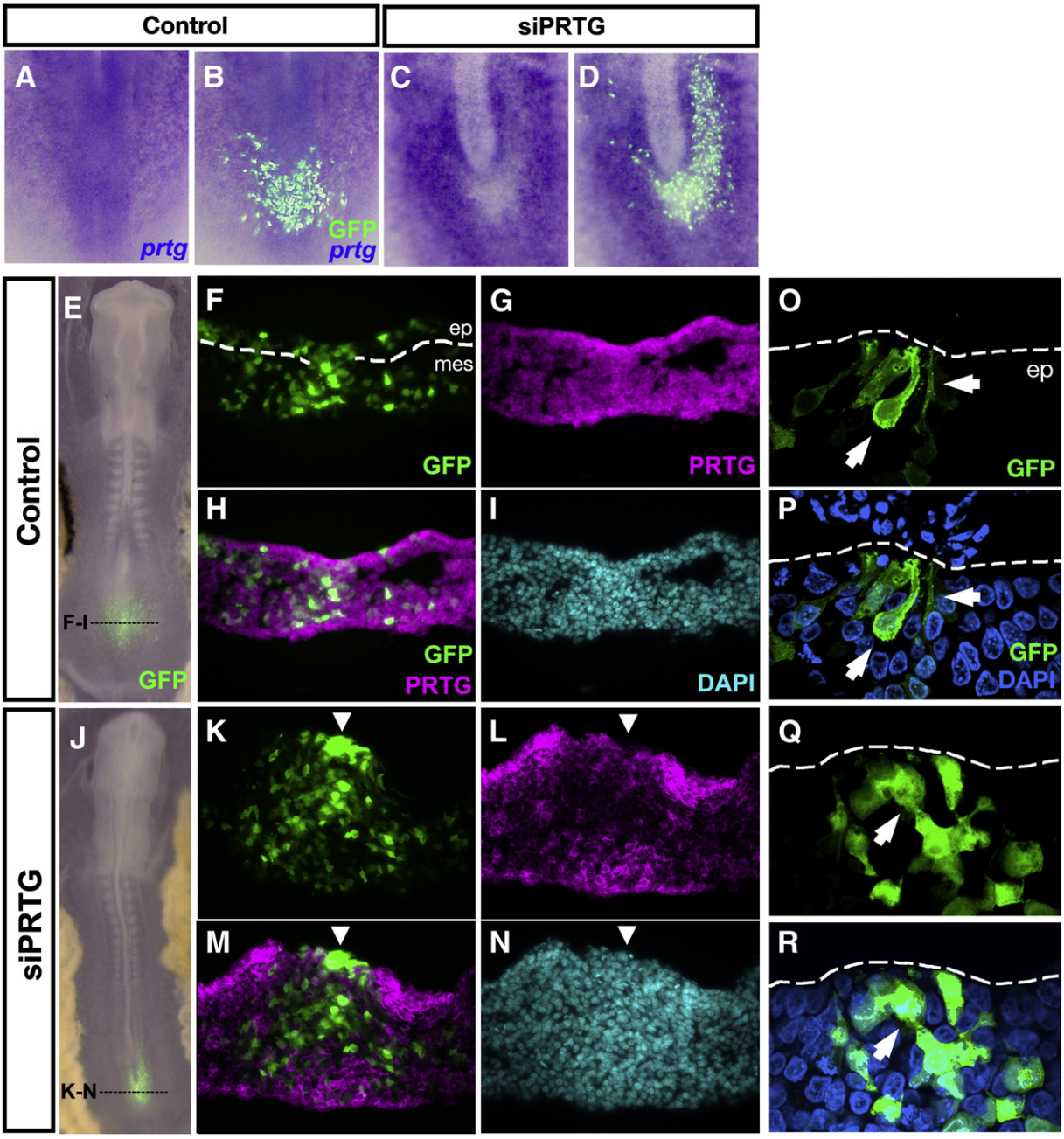

Fig. 5. Knockdown of Protogenin (PRTG) by double-stranded siRNA. Control five-base mismatched siRNA (Control) or siRNA targeted for PRTG (siPRTG) was co-electroporated with pCAGGS-EGFP. (A-D) Expression of *prtg* mRNA 6 h after electroporation. In vitro electroporation was performed on embryos at stage 6 embryos that were then incubated for further 6 h by whole embryo culture. Although *prtg* expression was intact after control siRNA transfection (A, B), it was significantly reduced following siPRTG transfection (C, D). (E–N) Expression of PRTG protein 12 h after electroporation. In ovo electroporation was performed on stage 7 embryos. Dotted lines in (E) and (J) denote the level of the transverse sections in (F–I) and (K–N). The white dotted line in (F) divides the epiblast and mesodermal layer. Although control siRNA did not affect PRTG protein expression (F–I), siPRTG decreased PRTG expression significantly (K–N). Note the accumulation of GFP positive/PRTG negative cells at the primitive streak (K–N; white arrowhead). (O–R) Confocal image of the transfected cells on the apical side of the epiblast. White dotted lines denote the apical surface of the epiblast. Whereas the transfected cells with the control siRNA exhibited a polarized shape, that with siPRTG had round morphology (white arrows). ep, epiblast; mes, mesoderm.

Loss-of-function for PRTG deforms the paraxial mesoderm

The effects of PRTG-knockdown on the paraxial mesoderm were further examined at 28 h after electroporation. The anterior limit of GFP-expressing cells was not affected by PRTG-knockdown, although the width of the GFP expression array became narrower (cf. Fig. 7A and E). GFP-expressing cells in PRTG-knockdown embryos were located in both the somite and presomitic mesoderm, as in control embryos (Fig. 7A', E'), indicating that the migration of these paraxial mesodermal cells was not perturbed by PRTG-knockdown. However, in the somites and presomitic mesoderm that were composed mainly of PRTG-knockdown cells, cavities were formed (Fig. 7F-F", G-G"). Somites in the control embryos exhibited an epithelial structure: that is, the somites consisted of columnar cells tightly adhered to each other (Fig. 7D). In contrast, somites in PRTG-knockdown embryos were comprised of flattened cells, and the intercellular contacts were not so tight as that in the control group (Fig. 7H). It appears that somite cells in PRTG-knockdown embryos could not maintain their epithelial structure. (cf. Fig. 7D and H). In PRTG-knockdown embryos, clusters of GFP-expressing cells were periodically arranged in the presomitic mesoderm (Fig. 7E'). In transverse sections, the clusters were located in the medioventral part of the presomitic mesoderm

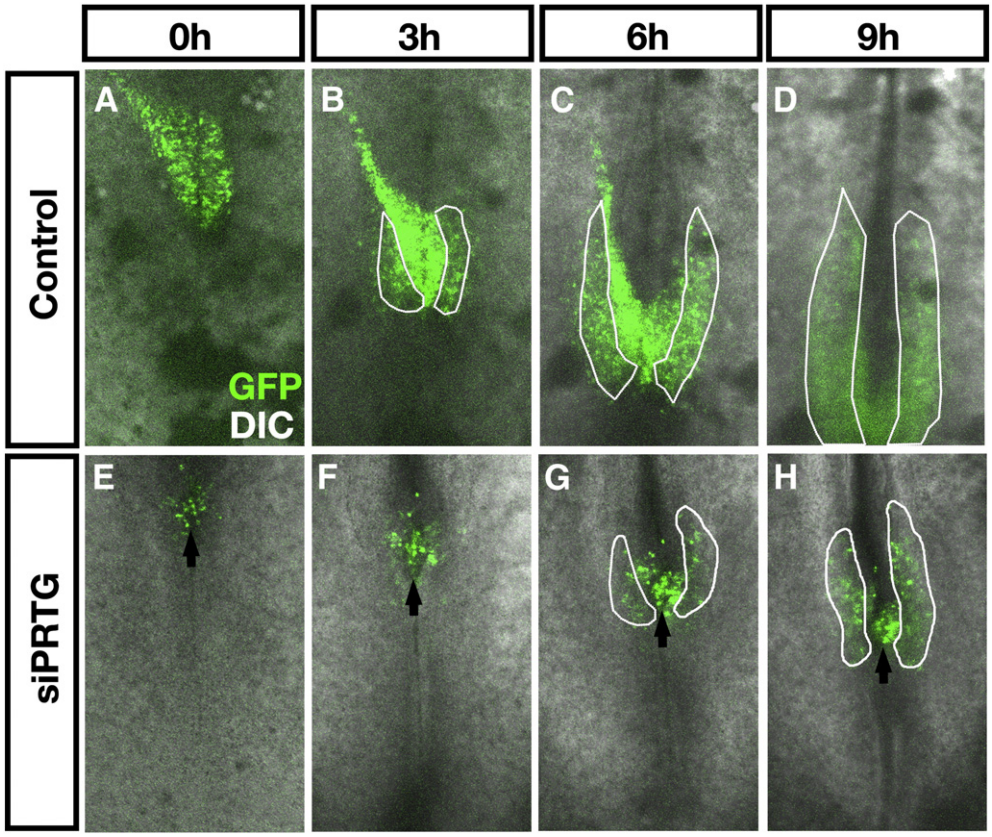

Fig. 6. Time-lapse imaging of double-stranded siRNA knockdown in in vitro whole embryo culture. Control siRNA (Control; A–D) or siRNA targeted for PRTG (siPRTG; E–H) was co-electroporated with pCAGGS-EGFP. Images capturing started 3.5 h after electroporation when GFP fluorescence was clearly detectable. Z-stack images of GFP and DIC were merged to show 3-h interval from Movie 1 and Movie 2. The upper panel (A–D) shows that control siRNA-transfected cells ingressed and moved anterolaterally to join the array of the paraxial mesoderm (white enclosure; two similar phenotypes from two independent experiments). The lower panel (E–H) shows that some PRTG-knockdown cells did not ingress (black arrow; five similar phenotypes from five independent experiments).

(Fig. 7G, G'). It was confirmed that PRTG expression was down-regulated in the transfected cells comprising the clusters (Fig. 7I–I") and the cavernous somites (Fig. 7J–J").

Finally, a rescue experiments were performed by cotransfection of mutated *prtg* cDNA with synonymous substitution at the target sequence for siRNA, which is not sensitive to siPRTG. In these embryos, the number of clusters was reduced (in one of five embryos) or abolished (four of five embryos; Fig. 7K, K'), and cellular arrangements in the presomitic mesoderm (Fig. 7M–M") and somite (Fig. 7L–L", N) were restored (in five of five embryos). These results indicate that loss-of-function for PRTG does not affect mesodermal migration, although it does disrupt tissue integration of the paraxial mesoderm.

Discussion

In the present study, we examined the role of PRTG in the rearrangement of cells of the paraxial mesodermal lineage during early chick embryogenesis. Using an in vitro aggregation assay, we found that PRTG augmented the adhesive properties of cultured L-cells. Furthermore, *prtg* mRNA and protein were expressed continuously by cells of the paraxial mesodermal lineage, with precursor cells remaining in the epiblast until they formed somites. PRTG protein was localized to sites of contact between cells in the epiblast, as well as migrating paraxial mesodermal cells. Overexpression of PRTG resulted in the formation of cell aggregates and a delay in mesodermal cell migration. Finally, PRTG-knockdown impaired the ingression of paraxial mesoderm precursor cells, as well as disrupting tissue organization of the paraxial mesoderm, producing cavernous somites and multiple clusters of cells. Based on these results, various roles of PRTG are suggested, as discussed below.

PRTG is a member of the IgSF with immunoglobulin-like domains and fibronectin III repeats in the extracellular region. Closely related molecules include neural cell adhesion molecules such as L1 and NCAM, which mediate cell–cell adhesion through homophilic binding and are also involved in heterophilic interactions with the ECM. In this regard, PRTG may function as an adhesion molecule. Indeed, the results of the in vitro aggregation assay indicate that PRTG can function as a cell adhesion molecule through homophilic binding. Because PRTG was localized at the sites of contact between cells, we assume that PRTG provides traction, enabling ingressing or migrating cells to move. It has been shown previously that homophilic binding of the adhesion molecule N-cadherin generates traction force in vitro (Ganz et al., 2006).

In experiments evaluating the effects of PRTG overexpression, PRTG-overexpressing cells formed aggregates, supporting the notion that PRTG mediates homophilic cell–cell adhesion. PRTG-transfection may have conferred higher adhesive properties to presumptive mesodermal cells; that is, cells become sticky. Consequently, mesodermal cell migration may have been interfered with such that the anterior limit of the PRTG-overexpressing cells that participated in somitogenesis became more caudal compared with that seen in the control embryos (Fig. 3F, G). The movement of individual mesodermal cells after ingression is most active in the early phase of mediolateral migration away from the primitive streak, which decreases gradually as the mesodermal cells join the paraxial mesoderm (Zamir et al., 2006). In the present study, the acquisition of greater adhesive properties may have resulted in the formation of aggregates, and interfered with the migration of these cells. Consequently, the

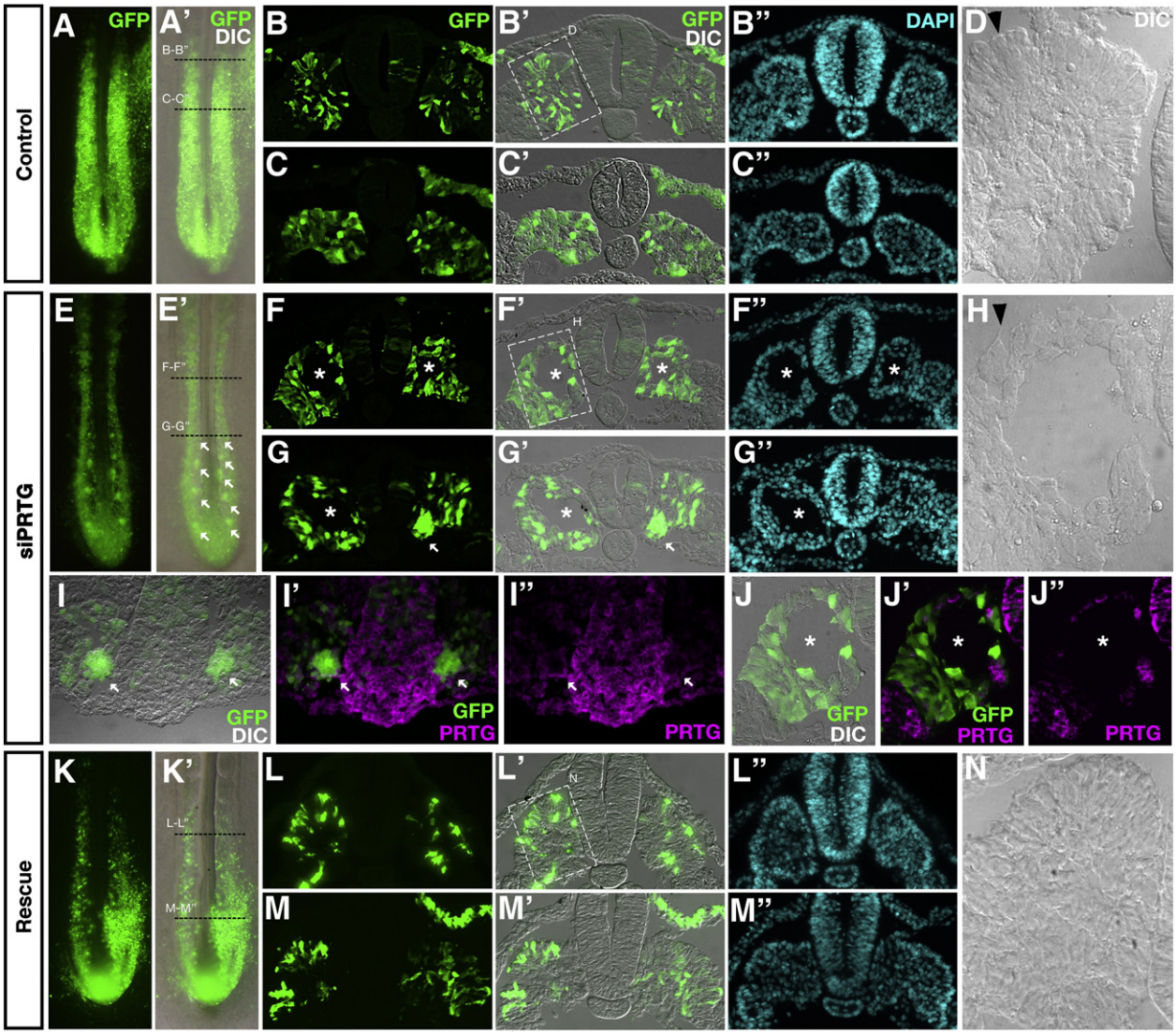

Fig. 7. Knockdown of Protogenin (PRTG) deforms the paraxial mesoderm. Results obtained 28 h after co-electroporation of control five-base mismatched siRNA (Control; A–D) or siRNA targeted for PRTG (siPRTG; E–J) or siPRTG and pCAGGS-PRTGmut (Rescue; K–N) with pCAGGS-EGFP. Dotted lines in A', E', and K' denote the level of the transverse sections. Higher magnification images of boxes in B', F', and L' are shown in D, H, and N. Control siRNA-transfected cells were dispersed ubiquitously throughout the somites and the presomitic mesoderm (B–B", C–C"; three similar phenotypes from three independent experiments). Cavities were formed in the middle of siPRTG-transfected somites and the presomitic mesoderm, as denoted by asterisks (F'–F", G–G"; five similar phenotypes from five independent experiments). Although control siRNA-transfected somitic epithelial cells exhibit an orderly epithelial morphology (D; an arrowhead), siPRTG-transfected cells in equivalent position were deformed and lost their epithelial morphology (H; an arrowhead). The siPRTG-transfected cells formed cell aggregates at the medioventral part of the presomitic mesoderm (G–G"; arrows; four similar phenotypes from five independent experiments). PRTG expression was decreased in the cell aggregates (I–I"; arrows) and somites (J–J") after transfection of siPRTG. Addition of siPRTG-insensitive PRTG construct to siPRTG rescued the phenotype with cell aggregates (K–K', M–M"; four similar phenotypes from five independent experiments) and restored normal somite formation (L–L", N; five similar phenotypes from five independent experiments).

participation of the migrating cells to the paraxial array was delayed and the transfected cells were observed to be distributed caudally in the paraxial mesoderm. Nevertheless, the total number of somites in PRTG-overexpressing embryos did not differ from that in the control embryos, although smaller somites were observed in PRTG-overexpressing embryos. These results suggest delayed migration of mesodermal cells may have not interfered with the segmentation clock.

In loss-of-function experiments, PRTG-knockdown cells remained in the epiblast, accumulating near the primitive streak at 12 h after electroporation (Fig. 5J–N). Perturbed ingression of PRTG-knockdown cells was also observed in time-lapse analysis (Fig. 6E–H; Movie 2). These results indicate that PRTG-mediated adhesion is required for the ingression of epiblast cells. On the apical side of the epiblast, PRTG-knockdown cells exhibited a round morphology, losing their epithelial shape or the bottle shape associated with ingressing cells (Fig. 5Q). Without PRTG-mediated adhesion, these cells may not have maintained cell–cell contact and thus lost the cell polarity required for directional migration. Of the other adhesion molecules, E-cadherin expressed in the epiblast is required for epithelial formation, and its downregulation is necessary for ingression (Hatta and Takeichi, 1986; Nieto et al., 1994; Cano et al., 2000; Zohn et al., 2006). N-cadherin, which replaces E-cadherin upon ingression, is not required for ingression, although it is necessary for mesodermal migration and morphogenesis (Radice et al., 1997; Yang et al., 2008). In siRNA experiment, however, E-cadherin expression in the epiblast was not perturbed (data not shown). Therefore, these cadherins are not enough to mediate the traction necessary in PRTG-knockdown cells to ingress. Although PRTG-knockdown cells may have lost traction in the epiblast, intact epiblast cells move lateromedially to the primitive streak, thereby pushing the PRTG-knockdown cells. The PRTG-knockdown cells then accumulate at the primitive streak, eventually

falling down the streak as a mass when a certain number of cells has accumulated. Because embryos are extending continuously, the fallen cell mass may be arranged periodically in the presomitic mesoderm, as indicated in Fig. 7E. The caudal distribution of this cell mass in the array of the paraxial mesoderm supports the notion that the ingression of PRTG-knockdown cells was delayed. In this regard, we propose that PRTG-mediated adhesion is required to support the continuous ingression of the cells.

Although some PRTG-knockdown cells were stacked in the epiblast, some cells had ingressed and were located under the epiblast at 12 h after electroporation (Fig. 5K). These cells may have lost PRTG after their ingression as a result of a time lag in the effects of the siRNA. Although the width of the GFP belt in PRTG-knockdown cells is narrower than in the control group, the rostral limit of PRTG-knockdown group did not differ from control (Fig. 7A, E). PRTG-knockdown cells eventually contributed to somite formation, without delay, at 28 h after electroporation. These results indicate that PRTG is not involved in mesodermal cell migration after the cells have ingressed. It has been reported that N-cadherin is required for mesodermal cell migration under the control of platelet-derived growth factor (PDGF) signaling (Yang et al., 2008). Because the expression of N-cadherin in paraxial mesoderm was not affected after PRTG-knockdown (data not shown), N-cadherin-mediated adhesion may be sufficient to drive the migration. Alternatively, the partial loss of cell adhesion may not significantly affect migration because mesodermal cell migration is mostly due to convective tissue movement, and mesodermal cells move cell-autonomously independent of tissue movements (Zamir et al., 2006; Bénazéraf et al., 2010).

In the paraxial mesoderm of PRTG-knockdown embryos, although somite numbers were not affected (data not shown), huge cavities were formed in the presomitic mesoderm (Fig. 7G–G'') and somites (Fig. 7F–F''). In particular, the somite cells could not form an orderly arranged epithelial structure, and lost their intercellular contacts (Fig. 7H). It is known that the somitic cells have a high adhesive property (Bellairs et al., 1978; Cheney and Lash, 1984). Considering the high level of PRTG expression at the center of the somite, re-epithelialization of the mesenchymal cells to form epithelial somites may be disturbed after loss of PRTG-mediated adhesion, resulting in disorganized somites with cavities. Similar, but not identical, epithelial disorganization of the somites has been reported in mice lacking N-cadherin; these somites were small and less cohesive (Radice et al., 1997) and the disorganization was enhanced by further loss of cadherin-11 (Horikawa et al., 1999). Therefore, adhesion generated by cadherins may not be enough to maintain epithelial structure of somites and the loss of PRTG may disrupt the epithelial structure of somites. In the presomitic mesoderm, although mesenchymal cells are less adhesive than epithelial somite cells in dissociated culture, they maintain intercellular contact in vivo, as revealed by electron microscopy (Trestad et al., 1967; Bancroft and Bellairs, 1975). Because PRTG is localized at the sites of contact (Fig. 2I), PRTG-knockdown may have disrupted tissue integrity. Considering these findings together, we propose that PRTG-mediated adhesion is required for the proper tissue organization of the paraxial mesoderm. However, in PRTG-knockdown embryos, somite segmentation proceeded in a timely manner because the total number of somites was comparable to that in the control group. Therefore, the oscillation network and segmentation mechanisms are independent of individual cell adhesiveness mediated by PRTG.

Although we have discussed the roles for PRTG in line with cell adhesion, our results don't exclude the possibility of other underlying function of PRTG. Some IgSF molecules including L1 and NCAM, which exert adhesive activity via trans-binding as PRTG, can cis-interact with other transmembrane receptor to form receptor complex (Doherty and Walsh, 1996; Brümmendorf and Lemmon, 2001). PRTG belongs to similar IgSF to L1 and NCAM, and it may also form receptor complex. In this context, loss of PRTG may affect such complex and change intracellular signaling, which may result in change of cell fate and behaviors. PRTG-knockdown cells in the epiblast may have lost epithelial identity before ingression, stacked as different cell identity among the epiblast and eventually they were pushed by intact epiblast cells to form cell clusters (Figs. 5K and 7I). Alternatively, PRTG-knockdown cells may have failed in epithelial to mesenchymal transition and kept epithelial identity among the presomitic mesoderm to form cell clusters.

It was reported recently that PRTG can function as a receptor to bind a putative diffusible ligand and suppress premature neuronal differentiation during early neural development (Wong et al., 2010). Although it is not known whether PRTG in the mesoderm can function in a manner similar to that of a receptor, our results on the roles of PRTG in adhesion cannot be explained by its receptor function. PRTG may have multiple functions depending upon cell lineage and environment.

In conclusion, our results suggest that PRTG plays a role in facilitating the adhesiveness of cells of the paraxial mesodermal lineage and is required for the successive ingression of these cells. We propose that PRTG may be also necessary for supporting tissue integrity of the paraxial mesoderm for re-epithelialization.

Supplementary materials related to this article can be found online at doi:10.1016/j.ydbio.2010.11.024.

Acknowledgments

The authors thank Drs. Yoshiko Takahashi and Koichi Kawakami for Tol2 transposon system. We also thank to Emiko Kurokawa and Yukari Mizuta for technical assistance. This study was supported by Grants-in-Aid for Scientific Research (C) from the Japan Society for the Promotion of Science (JSPS) to Y.W.

References

Bancroft, M., Bellairs, R., 1975. Differentiation of the neural plate and neural tube in the young chick embryo. Anat. Embryol. 147, 309–335.
Bellairs, R., Curtis, A.S.G., Sanders, E.J., 1978. Cells dissected from segmented mesoderm were found to be more adhesive than cells from unsegmented mesoderm. J. Embryol. exp. Morph. 46, 207–213.
Bellairs, R., 1979. The mechanism of somite segmentation in the chick embryo. J. Embryol. exp. Morph. 51, 227–243.
Bénazéraf, B., Francois, P., Baker, R.E., Denans, N., Little, C.D., Pourquié, O., 2010. A random cell motility gradient downstream of FGF controls elongation of an amniote embryo. Nature 466, 248–252.
Brümmendorf, T., Lemmon, V., 2001. Immunoglobulin superfamily receptors: cis-interactions, intracellular adapters and alternative splicing regulate adhesion. Curr. Opin. Cell Biol. 13, 611–618.
Burdsal, C.A., Damsky, C.H., Pedersen, R.A., 1993. The role of E-cadherin and integrins in mesoderm differentiation and migration at the mammalian primitive streak. Development 118, 829–844.
Cano, A., Perez-Moreno, M.A., Rodrigo, I., Locascio, A., Blanco, M.J., del Barrio, M.G., Portillo, F., Nieto, M.A., 2000. The transcription factor snail controls epithelial–mesenchymal transitions by repressing E-cadherin expression. Nat. Cell Biol. 2, 76–83.
Catala, M., Teillet, M.-A., De Robertis, E.M., Le Douarin, N.M., 1996. A spinal cord fate map in the avian embryo: while regressing, Hensen's node lays down the notochord and floor plate thus joining the spinal cord lateral walls. Development 122, 2599–2610.
Chapman, S., Collignon, J., Schoenwolf, G., Lumsden, A., 2001. Improved method for chick whole-embryo culture using a filter paper carrier. Dev. Dyn. 220, 284–289.
Cheney, C.M., Lash, J.W., 1984. An increase in cell–cell adhesion in the chick segmental plate results in a meristic pattern. J. Embryol. exp. Morph. 79, 1–10.
Ciruna, B., Rossant, J., 2001. FGF signaling regulates mesoderm cell fate specification and morphogenetic movement at the primitive streak. Dev. Cell 1, 37–49.
Doherty, P., Walsh, F.S., 1996. CAM-FGF receptor interactions: a model for axonal growth. Mol. Cell. Neurosci. 8, 99–111.
Ganz, A., Lambert, M., Saez, A., Silberzan, P., Buguin, A., Mège, R.M., Ladoux, B., 2006. Traction forces exerted through N-cadherin contacts. Biol. Cell 98, 721–730.
Hamburger, V., Hamilton, H.L., 1951. A series of normal stages in the development of the chick embryo. J. Morphol. 88, 49–92.
Hammerschmidt, M., Wedlich, D., 2008. Regulated adhesion as a driving force of gastrulation movements. Development 135, 3625–3641.
Hatakeyama, J., Shimamura, K., 2008. Method for electroporation for the early chick embryo. Dev. Growth Diff. 50, 449–452.
Hatta, K., Takeichi, M., 1986. Expression of N-cadherin adhesion molecules associated with early morphogenetic events in chick development. Nature 320, 447–449.
Henrique, D., 1997. In situ hybridization on cryostat sections of chick embryos. In: Jowett, T. (Ed.), Tissue in situ hybridization. John WileyandSons, Inc. and Spektrum Akademischer Verlag, pp. 73–75.

Horikawa, K., Radice, G., Takeichi, M., Chisaka, O., 1999. Adhesive subdivisions intrinsic to the epithelial somites. Dev. Biol. 215, 182–189.
Iimura, T., Yang, X., Weijer, C., Pourquié, O., 2007. Dual mode of paraxial mesoderm formation during chick gastrulation. Proc. Natl Acad. Sci. USA 107, 2744–2749.
Larue, L., Ohsugi, M., Hirchenhain, J., Kemler, R., 1994. E-cadherin null mutant embryos fail to form a trophectoderm epithelium. Proc. Natl Acad. Sci. USA 91, 8263–8267.
Nakaya, Y., Sukowati, E.W., Wu, Y., Sheng, G., 2008. RhoA and microtubule dynamics control cell–basement membrane interaction in EMT during gastrulation. Nat. Cell Biol. 10, 765–775.
Nieto, M.A., Sargent, M.G., Wilkinson, D.G., Cooke, J., 1994. Control of cell behavior during vertebrate development by Slug, a zinc finger gene. Science 264, 835–839.
Ooi, V.E.C., Sanders, E.J., Bellairs, R., 1986. The contribution of the primitive streak to the somites in the avian embryo. J. Embryol. exp. Morph. 92, 193–206.
Psychoyos, D., Stern, C.D., 1996. Fates and migratory routes of primitive streak cells in the chick embryo. Development 122, 1523–1534.
Radice, G.L., Rayburn, H., Matsunami, H., Knudsen, K.A., Takeichi, M., Hynes, R.O., 1997. Developmental defects in mouse embryos lacking N-cadherin. Dev. Biol. 181, 64–78.
Rifes, P., Carvalho, L., Lopes, C., Andrade, R.P., Rodrigues, G., Palmeirim, I., Thorsteinsdóttir, S., 2007. Redefining the role of ectoderm in somitogenesis: a player in the formation of the fibronectin matrix of presomitic mesoderm. Development 134, 3155–3165.
Sato, Y., Yasuda, K., Takahashi, Y., 2002. Morphological boundary forms by a novel inductive event mediated by Lunatic fringe and Notch during somatic segmentation. Development 129, 3633–3644.
Sato, Y., Kasai, T., Nakagawa, S., Tanabe, K., Watanabe, T., Kawakami, K., Takahashi, Y., 2007. Stable integration and conditional expression of electroporated transgenes in chicken embryos. Dev. Biol. 305, 616–624.
Schoenwolf, G.C., Garcia-Martinez, V., Dias, M.S., 1992. Mesoderm movement and fate during avian gastrulation and neurulation. Dev. Dyn. 193, 235–248.
Toyoda, R., Nakamura, H., Watanabe, Y., 2005. Identification of protogenin, a novel immunoglobulin superfamily gene expressed during early chick embryogenesis. Gene Expr. Patterns 5, 778–785.
Trestad, R.L., Hay, E.D., Revel, J.-P., 1967. Cell Contact during Early Morphogenesis in the Chick Embryo. Dev. Biol. 16, 78–106.
Vesque, C., Anselme, I., Couvé, E., Charnay, P., Schneider-Maunoury, S., 2006. Cloning of vertebrate Protogenin (Prtg) and comparative expression analysis during axis elongation. Dev. Dyn. 235, 2836–2844.
Warga, R.M., Kane, D.A., 2007. A role for N-cadherin in mesodermal morphogenesis during gastrulation. Dev. Biol. 310, 211–225.
Wilson, V., Beddington, R.S.P., 1996. Cell fate and morphogenetic movement in the late mouse primitive streak. Mech. Dev. 55, 79–89.
Wong, Y.-H., Lu, A.-C., Wang, Y.-C., Cheng, H.-C., Chang, C., Chen, P.-H., Yu, J.-Y., Fann, M.-J., 2010. Protogenin defines a transition stage during embryonic neurogenesis and prevents precocious neural differentiation. J. Neurosci. 30, 4428–4439.
Yang, X., Chrisman, H., Weijer, C.J., 2008. PDGF signalling controls the migration of mesoderm cells during chick gastrulation by regulating N-cadherin expression. Development 135, 3521–3530.
Zamir, E.A., Czirók, A., Cui, C., Little, C.D., Rongish, B.J., 2006. Mesodermal cell displacements during avian gastrulation are due to both individual cell-autonomous and convective tissue movements. Proc. Natl Acad. Sci. USA 103, 19806–19811.
Zohn, I.E., Li, Y., Skolnik, E.Y., Anderson, K.V., Han, J., Niswander, L., 2006. p38 and a p38-interacting protein are critical for downregulation of E-cadherin during mouse gastrulation. Cell 125, 957–969.